Acta
Biologica
Szegediensis

ARTICLE

Structure-based assortment of herbal analogues against spike protein to restrict COVID-19 entry through hACE2 receptor: An *in-silico* approach

Sourav Santra[1#], Sasti Gopal Das[1#], Suman Kumar Halder[2], Kuntal Ghosh[3], Amrita Banerjee[4], Amiya Kumar Panda[1,5] and Keshab Chandra Mondal[1,2]*

[1]BIF Center, Vidyasagar University, Midnapore-721102, West Bengal, India
[2]Department of Microbiology, Vidyasagar University, Midnapore-721102, West Bengal, India
[3]Department of Biological Sciences, Midnapore City College, Midnapore-721129, West Bengal, India
[4]Department of Biotechnology, Oriental Institute of Science & Technology, Midnapore-721102, West Bengal, India
[5]Department of Chemistry and Chemical Technology, Vidyasagar University, Midnapore-721102, West Bengal, India

ABSTRACT On-going global pandemic COVID-19 has spread all over the world and has led to more than 1.97 million deaths till date. Natural compounds may be useful to protecting health in this perilous condition. Mechanism of shuttle entry of SARS-COV-2 virus is by interaction with viral spike protein with human angiotensin-converting enzyme-2 (ACE-2) receptor. To explore potential natural therapeutics, 213 important phytochemicals of nine medicinal plants *Aconitum heterophyllum, Cassia angustifolia, Cymbopogon flexuosus, Cymbopogon martinii, Nux vomica, Phyllanthus urinaria, Swertia chirayita, Justicia adhatoda, Vetiveria zizanioides* were selected for in-silico molecular docking against the spike protein of SARS-COV-2 and compared with recently prescribed drug chloroquine, ramdesivir, lopinavir and hydroxychloroquine. Results revealed that rhamnocitrin of *P. urinaria*, 1,5-dihydroxy-3,8-dimethoxyxanthone of *S. chirayita* and laevojunenol of *V. ziza-nioides* potentially binds with the receptor binding site of SARS-COV-2 spike glycoprotein and more robustly destabilized the RBD-ACE-2 binding over chloroquine, ramdesivir, lopinavir and hydroxychloroquine. It was also found that laevojunenol, rhamnocitrin, and 1,5-dihydroxy-3,8-dimethoxyxanthone qualified the criteria for drug-likeness as per Lipinski rule. After attachment of the selected phytochemical with the spike protein the affinity of the later towards ACE-2 was minimized and the effect of 1,5-dihydroxy-3,8-dimethoxyxanthone and laevojunenol was superior. Hence, rhamnocitrin of *P. urinaria*, 1,5-dihydroxy-3,8-dimethoxyxanthone of *S. chirayita* and laevojunenol of *V. zizanioides*, are potential therapeutic molecules for SARS-COV-2, which upon binding with spike protein changes the affinity of the spike towards ACE-2 and therefore restrict the entry of the virus into a human cell. Subsequent clinical validation is needed to confirm these phytochemicals as drugs to combat COVID-19. **Acta Biol Szeged 64(2):159-171 (2020)**

INTRODUCTION

Presently, the world's population is in under tremendous pressure, due to COVID-19 pandemic. Worldwide, more than 90 million people are infected and among them more than 1.97 million people died till date (as per WHO). Deaths are increasing by leaps and bounds due to community transmission and the scientists are deliberately trying to find drugs from natural and synthetic origin to use as a potential antiviral agent. The entry of the COVID-19 virus into human cells is mediated via transmembrane spike (S) glycoprotein that contributes to the cell receptor binding, tissue tropism, and pathogenesis. Spike protein has conserved motifs have three domains

namely S1, S2 and N. The S1-domain has a conserved receptor-binding domain (RBD), which recognizes the angiotensin-converting enzyme-2 (ACE-2) receptor (Bourgonje et al. 2019; Yao et al. 2020) which is the initial step of entry mechanism into the host cells (Walls et al. 2020; Wang et al. 2020). The expression of ACE-2 is higher in the intestinal epithelium and pulmonary pneumocytes than other tissues. The interaction of S protein and ACE-2 results in imbalance of the renin-angiotensin system in the lungs as well as immunological intolerance, which leads to acute lung injury such as pulmonary oedema (Yao et al. 2020; Yang et al. 2007; Kuba et al. 2005). The entry of coronavirus into susceptible cells is a complex process that requires the concerted action of receptor binding and proteolytic processing of the S protein,

# Both the authors contributed equally.

which endorses virus-cell fusion (Walls et al. 2020). In recent time, chloroquine, hydroxychloroquine, remdesivir, lopinavir, arbidol are drugs of choice for COVID treatment but they have limitations and side effects (Wang et al. 2020; Cao et al. 2007; Rismanbaf et al. 2020; Yazdany et al. 2020). Under this emergency, several conventional and non-conventional medicines are being tested around the world to restrict viral transmission and to develop effective therapeutics. In this perspective, medicinal plants especially those employed in traditional medicine for the treatments of virus-allied symptoms have recently come under scientific surveillance as they contain bioactive compounds that could be useful for development of potential drugs against COVID like viral diseases.

Since ancient human civilization, many phytochemicals of diversified unique properties are being explored for customized treatments of variety of diseases owing to their analgesic, antipyretic, antioxidative, anticancer, immunomodulatory, anti-inflammatory, antimicrobial, anti-carcinogenic and many other notable properties (Jaiswal and Williams 2017; Suresh and Abraham 2020; Koparde et al. 2019). In global perspective, Lion's share of the world population still depends on plant derived products to formulate drugs to treat their health problems. Some selective herbal products have low cytotoxicity and high bioavailability and are effective for the treatment of different viral diseases (Divya et al. 2020). The potential biological roles of plant's secondary metabolites have now been explored in the blockage of virus particle's entry, their multiplication and pathogenesis (ul Qamar et al. 2020). Among the different plants, *P. urinaria* (commonly called gripe weed) have potential ethnomedicinal importance against asthma, bronchitis, cough, tuberculosis, fever, influenza, digestive pain, conjunctivitis and anaemia. Besides, this plant also effective against hepatitis A-C, herpes and HIV (Singh 2018). *S. chirayita* (also is known as *chirayta*) is useful for the cure of different diseases and containing anti-inflammatory, antioxidant and antiviral compounds. *S. chirayita* has also very good antiviral activity against herpes and papilloma virus (Singh 2018; Kumar and Van Staden 2016). Likewise, *V. zizanioides* (vetivergrass; Hindi: Khas-Khas) used to treat many skin and nervous disorders and claimed to inhibit the dengue NS2B–NS3 virus (Lavanya et al. 2016). *A. heterophyllum* also helps in the treatment of common cold, flu, and malaria bronchitis, persistent cough and upper respiratory tract infections (Paramanick et al. 2017). *C. flexuosus* commonly used against headaches, diabetes, rheumatism, hypertension, wounds, fever and bone fractures (Rajeswara Rao 2013). *Nux vomica* is used against colds and flu, particularly in the early stages of any virus infection (Singh 2018). These all plants are selected based on their ethno-botanical importance and the study

Table 1. Synthetic compounds and their binding energy with SARS-COV-2 spike glycoprotein.

SI No.	Compound names	Binding energy (kcal/mol)
1	Ramdesivir	-8.1
2	Lopinavir	-11.8
3	Chloroquine	-6.7
4	Hydroxychloroquine	-6.6

of literature. The present study was aimed to explore the interaction of natural compounds of *A. heterophyllum, C. angustifolia, C. flexuosus, C. martinii, N. vomica, P. urinaria, S. chirayita, J. adhatoda, V. zizanioides* with the spike protein of the SARS-CoV-2 virus. The 3D structure of S protein was constructed and its binding ability against the 213 phytochemicals of the above-mentioned medicinal plants were evaluated. The post binding effect of the conjugated spike protein with ACE-2 was also addressed in order to explore the effectiveness of natural compounds as potential anti-COVID drug.

MATERIALS AND METHODS

Retrieval of protein sequence and prediction of homologous structure

The reference spike glycoprotein YP_009724390.1 sequence of human corona virus SARS-COV-2 collected from NCBI. Three-dimensional structure of corona viral spike glycoprotein (PDB ID: 6VSB) and human Angiotensin Converting Enzyme-2 (ACE-2) (PDB ID: 4APH) were retrieved from RCSB Protein Data Bank (https://www.rcsb.org/) in PDB format and modelling of the spike glycoprotein (YP_009724390.1) was carried out in SWISS-MODEL server (Waterhouse et al. 2018) and further analysed by using PyMol (DeLano 2002). Quality assessment of this spike glycoprotein model was validated by PROCHECK by analysing the Ramachandran plot (Laskowski et al. 1993).

Retrieval of ligands structure

Three-dimensional structure of 213 natural compounds of *A. heterophyllum, C. angustifolia, C. flexuosus, C. martinii, N. vomica, P. urinaria, S. chirayita, J. adhatoda, V. zizanioides* and drugs remdesivir, lopinavir, chloroquine and hydroxychloroquine was retrieved from Indian Medicinal Plants, Phytochemistry and Therapeutics (IMPPAT) database (Mohanraj et al. 2018), PubChem (Kim et al. 2016) on the basis of literature survey and listed in Table 1-3.

Protein-ligand docking

Prior docking, the water molecules were removed from the

Table 2. List of natural plant derived compounds whose binding energy is higher than -7 kcal/mol when binds with SARS-COV-2 spike glycoprotein.

No	Compound names	Plant species	Binding energy (kcal/mol)	H-bond interaction
1	Hetidine	*A. heterophyllum*	-9.7	371
2	Isoatisine	*A. heterophyllum*	-8.7	-
3	Hetisinone	*A. heterophyllum*	-8.6	370, 489
4	Veratridine	*A. heterophyllum*	-8.5	115, 167
5	6-benzoylheteratisine	*A. heterophyllum*	-8.4	377, 379
6	Hetisine	*A. heterophyllum*	-8.4	370
7	Atidine	*A. heterophyllum*	-8.3	377, 379, 457
8	Beta-carotene	*A. heterophyllum*	-8.3	-
9	Atisine	*A. heterophyllum*	-8.2	455
10	Dihydroatisine	*A. heterophyllum*	-8.1	338, 339
11	Aricine	*A. heterophyllum*	-8	370, 457
12	Benzoylmesaconine	*A. heterophyllum*	-8	488
13	Lactone atisenol	*A. heterophyllum*	-8	457
14	Lappaconitine	*A. heterophyllum*	-7.6	357, 473, 475
15	6-acetylheteratisine	*A. heterophyllum*	-7.4	379
16	Heterophyllisine	*A. heterophyllum*	-7.4	489
17	Aconitine	*A. heterophyllum*	-7.3	-
18	Anisoylaconine	*A. heterophyllum*	-7.3	377, 457, 473
19	Hypaconitine	*A. heterophyllum*	-7.3	371, 373
20	Mesaconitine	*A. heterophyllum*	-7.3	371, 373
21	Phytosterols	*A. heterophyllum*	-7.3	457
22	Jesaconitine	*A. heterophyllum*	-7.2	165, 355
23	Isorhamnetin 3-gentiobioside	*C. angustifolia*	-8.4	369, 417, 457, 487, 489, 493
24	Kaempferol	*C. angustifolia*	-8.1	457, 477
25	Aloe-emodin	*C. angustifolia*	-7.7	457, 477
26	Tinnevellinglucoside	*C. angustifolia*	-7.6	371, 403, 409, 505
27	Sennaglucosides	*C. angustifolia*	-9.8	343, 370, 371, 453, 476, 478, 493
28	Emodin-8-glucoside	*C. angustifolia*	-8.9	369, 371, 375, 376, 405, 406, 409
29	Rhein	*C. angustifolia*	-8.6	-
30	Isorhamnetin	*C. angustifolia*	-8.6	457, 477
31	Arundoin	*C. flexuosus*	-8.7	-
32	Phytosterols	*C. flexuosus*	-7.8	457
33	Humulene	*C. flexuosus*	-7.5	457
34	Caryophylene oxide	*C. martinii*	-7	478
35	Stryvomicine A	*N. vomica*	-9.2	-
36	Beta-colubrine chloromethochloride	*N. vomica*	-8.8	457, 477
37	Alpha-colubrine chloromethochloride	*N. vomica*	-8.5	
38	Oleanolic acid	*P. urinaria*	-8.7	370, 457
39	Trans-8,9-Dihydro-benz(a)anthracene-8,9-diol	*P. urinaria*	-8.7	-
40	Corilagin	*P. urinaria*	-8.7	379, 457, 487, 493
41	Naringin	*P. urinaria*	-8.7	343, 375, 403, 405, 437
42	Furosin	*P. urinaria*	-8.7	417, 456, 457, 493, 494
43	Kaempferol 7-methyl ether 4'-glucoside	*P. urinaria*	-8.7	417, 456, 457, 493, 494
44	Gallocatechingallate	*P. urinaria*	-8.6	457
45	Ellagic acid	*P. urinaria*	-8.5	371, 405, 408, 409
46	Cleistanthol	*P. urinaria*	-8.4	-
47	Quercetin	*P. urinaria*	-8.4	371, 455, 457, 477
48	Daucosterol	*P. urinaria*	-8.4	377, 488
49	Spruceanol	*P. urinaria*	-8.3	457, 490
50	Quercitrin	*P. urinaria*	-8.3	457, 488

Table 2. Continued.

No	Compound names	Plant species	Binding energy (kcal/mol)	H-bond interaction
51	13-Methyl-6,7,8,9,11,12,14,15,16,17-decahydrocyclopenta[a]phenanthrene-3,17-diol	*P. urinaria*	-8.2	-
52	Betulinic acid	*P. urinaria*	-8.2	408, 456, 457
53	Epigallocatechingallate	*P. urinaria*	-8.2	369, 379, 457, 487, 490
54	Rutin	*P. urinaria*	-8.2	372, 374, 375, 403, 405, 437, 439, 453, 505
55	Epicatechin-3-gallate	*P. urinaria*	-8.1	381, 417, 457, 487, 489
56	Beta-sitosterol	*P. urinaria*	-8.1	-
57	Glochidiol	*P. urinaria*	-8	408
58	Epicatechin	*P. urinaria*	-7.9	379, 381, 487, 489
59	Epigallocatechin	*P. urinaria*	-7.9	379, 381, 487, 489
60	Betulin	*P. urinaria*	-7.9	456, 457
61	Rhamnocitrin	*P. urinaria*	-7.9	379, 487, 489
62	Brevifolincarboxylic acid	*P. urinaria*	-7.8	375, 377, 415
63	Ethyl brevifolincarboxylate	*P. urinaria*	-7.5	371, 457, 477
64	Digallic acid	*P. urinaria*	-7.4	370, 457, 477, 478
65	Methyl brevifolincarboxylate	*P. urinaria*	-7.3	455, 457, 490
66	Urinatetralin	*P. urinaria*	-7.1	381
67	Episwertenol	*S. chirayita*	-9.7	-
68	Hopenol B	*S. chirayita*	-9.3	-
69	Erythrodiol	*S. chirayita*	-9.1	-
70	Friedlein	*S. chirayita*	-9.1	357
71	Chiratenol	*S. chirayita*	-8.9	-
72	Kairatenol	*S. chirayita*	-8.7	-
73	Swertanone	*S. chirayita*	-8.7	-
74	Oleanolic acid	*S. chirayita*	-8.6	-
75	Taraxasterol acetate	*S. chirayita*	-8.5	378, 408
76	Swertenol	*S. chirayita*	-8.3	466
77	Amarogentin	*S. chirayita*	-8.2	370, 371, 372, 457, 490
78	Swertiapuniside	*S. chirayita*	-8.1	372, 403, 439, 505, 506
79	Ursolic acid	*S. chirayita*	-8.1	457
80	1,8-Dihydroxy-2,6-dimethoxy-9H-xanthen-9-one	*S. chirayita*	-7.9	-
81	Mangiferin	*S. chirayita*	-7.9	379, 456, 457, 492
82	1,5-dihydroxy-3,8-dimethoxyxanthone	*S. chirayita*	-7.7	406, 409, 417
83	Swertianin	*S. chirayita*	-7.6	415, 377, 369
84	Decussatin	*S. chirayita*	-7.5	457, 477
85	Demethylbellidifolin	*S. chirayita*	-7.5	409
86	Isobellidifolin	*S. chirayita*	-7.5	371, 457
87	Swerchirin	*S. chirayita*	-7.5	371, 457
88	7,11-Epoxy-eremophila-1,9-dien-8-α-ol	*V. zizanioides*	-8.2	457
89	Eudesmane	*V. zizanioides*	-8	-
90	Cadalene	*V. zizanioides*	-7.9	-
91	Khusene	*V. zizanioides*	-7.9	-
92	10-epi-Acora-3,11-dien-15-al	*V. zizanioides*	-7.8	457, 478
93	Beta-vetivone	*V. zizanioides*	-7.8	457
94	15-nor-prezizaan-7-one	*V. zizanioides*	-7.7	457, 478
95	Isokhusimol	*V. zizanioides*	-7.7	457
96	Isovalencenol	*V. zizanioides*	-7.7	457, 477
97	Khusiol	*V. zizanioides*	-7.7	-
98	(1S,2S,8R)-2,6,7,7-tetramethyltricyclo[6.2.1.01,5] undecane	*V. zizanioides*	-7.7	-

Table 2. Continued.

No	Compound names	Plant species	Binding energy (kcal/mol)	H-bond interaction
99	Acora-2,4-diene	*V. zizanioides*	-7.6	-
100	Beta-cadinene	*V. zizanioides*	-7.6	-
101	Beta-vetivenene	*V. zizanioides*	-7.6	-
102	Khusimone	*V. zizanioides*	-7.6	-
103	Khusinol oxide	*V. zizanioides*	-7.6	478
104	7,15-epoxyprezizaane	*V. zizanioides*	-7.5	370
105	10-epi-Acor-3-en-5-one	*V. zizanioides*	-7.5	-
106	Allo-khusiol	*V. zizanioides*	-7.5	370
107	Alpha-vetispirene	*V. zizanioides*	-7.5	-
108	Eremophilane	*V. zizanioides*	-7.5	-
109	Khusilal	*V. zizanioides*	-7.5	457
110	Khusinodiol	*V. zizanioides*	-7.5	457
111	Khusitone	*V. zizanioides*	-7.5	-
112	13-nor-Eudesm-5-en-11-one	*V. zizanioides*	-7.4	457
113	Cedrane	*V. zizanioides*	-7.4	-
114	Epizizanal	*V. zizanioides*	-7.4	-
115	Isovetiselinenol	*V. zizanioides*	-7.4	-
116	Khusinol	*V. zizanioides*	-7.4	490
117	Laevojunenol	*V. zizanioides*	-7.4	489
118	11,12,13-tri-nor-cis-Eudesm-5-en-7-one	*V. zizanioides*	-7.3	-
119	Beta-Vetispirene	*V. zizanioides*	-7.3	-
120	Isokhusenic acid	*V. zizanioides*	-7.3	-
121	Isokhusinol oxide	*V. zizanioides*	-7.3	489
122	Nootkatone	*V. zizanioides*	-7.3	-
123	Cadin-4-en-10-ol	*V. zizanioides*	-7.2	-
124	Khusimol	*V. zizanioides*	-7.2	-
125	Ac1lb1ow	*V. zizanioides*	-7.1	-
126	Alpha-vetivone	*V. zizanioides*	-7.1	-
127	Cyclocopacamphenol	*V. zizanioides*	-7.1	457, 477
128	Epizizanone	*V. zizanioides*	-7.1	-
129	Khusol	*V. zizanioides*	-7.1	370

three-dimensional structure of the spike glycoprotein. The molecular docking study was performed for exploration of the binding affinity of the spike glycoprotein with the 213 selected natural phytochemicals in addition with remdesivir, lopinavir, chloroquine and hydroxychloroquine through AutoDock Vina [version 1.1.2] (Trott and Olson 2010). SARS-COV-2 spike protein S1 domain chains (A, B, C) have common reference active site of K417, G446, Y449, F486, N487, Y489, Q493, Q498, T500, N501, G502, Y505 (Walls et al. 2020; Wang et al. 2020; Yan et al. 2020; Lan et al. 2020). These sites were initially targeted for grid based molecular docking study with the selected natural phytochemicals. The grid box dimensions were 68 Å × 90 Å × 58 Å with a spacing of 1 Å and center set at coordinate 219.172, 224.276 and 287.134 in x, y, and z axis, respectively, centring around the ACE-2 binding domain. An array of ligands was screened based on binding energy at active site amino acid residues, and subsequently blindly docked with SARS-COV-2 spike protein using AutoDock with new grid dimension to cover the whole spike glycoprotein. The grid coordinate considered as 126 Å × 126 Å × 126 Å with a spacing of 1 Å and center set to coordinate 211.921, 226.209 and 247.631 in the x, y and z axis with 24 exhaustiveness, respectively. During blind docking, the size of grids was kept at maximum covering the whole surface of the protein to allow the ligand to bind in an unbiased binding pocket. Polar H charges of the Gasteiger-type were assigned to the receptor molecule and torsions were detected. Default settings of AutoDock Vina were used for docking studies.

Table 3. List of natural plant derived compounds whose binding energy is less than -7 kcal/mol when binds with SARS-COV-2 spike glycoprotein.

No	Compound names	Plant species	Binding energy (kcal/mol)
1	Phytosterols	*A. heterophyllum*	-6.9
2	Delphatines	*A. heterophyllum*	-6.7
3	Lycoctonine	*A. heterophyllum*	-6.6
4	Dl-borneol	*C. flexuosus*	-6
5	Citronellal	*C. flexuosus*	-5.7
6	Citral	*C. flexuosus*	-5.7
7	Methyleugenol	*C. flexuosus*	-5.6
8	Myrcene	*C. flexuosus*	-5.1
9	6-Methylhept-5-en-2-ol	*C. flexuosus*	-5
10	Triacontane	*C. flexuosus*	-4.9
11	Decanal	*C. flexuosus*	-4.8
12	Trans-2-Hepten-1-ol	*C. flexuosus*	-4.5
13	Beta-caryophyllene	*C. martinii*	-6.6
14	3-carene	*C. martinii*	-6.5
15	Carvylacetate	*C. martinii*	-6.4
16	P-cymene	*C. martinii*	-6.3
17	Alpha-terpineol	*C. martinii*	-6.3
18	Dihydrocarvone	*C. martinii*	-6.3
19	(-)-3-carene	*C. martinii*	-6.3
20	Beta-terpineol	*C. martinii*	-6.2
21	Perillyl alcohol	*C. martinii*	-6.2
22	D-carvone	*C. martinii*	-6.2
23	(-)-cis-carveol	*C. martinii*	-6.1
24	Cis,cis-farnesol	*C. martinii*	-6.1
25	Alpha-farnesene	*C. martinii*	-6.1
26	Limonene	*C. martinii*	-5.9
27	Eucalyptol	*C. martinii*	-5.8
28	Dihydrocarveol	*C. martinii*	-5.7
29	Geranyl acetate	*C. martinii*	-5.6
30	Geraniol	*C. martinii*	-5.3
31	6-Methyl-5-hepten-2-one	*C. martinii*	-5.2
32	6-Octen-1-ol, 3,7-dimethyl-, (R)-	*C. martinii*	-5.2
33	Geranyl butyrate	*C. martinii*	-5.1
34	(-)-Linalool	*C. martinii*	-4.9
35	2-Nonanol	*C. martinii*	-4.7
36	1,5-Hexadiyne	*J. adhatoda*	-5.4
37	2-(2,5-Hexadiynyloxy)tetrahydro-2H-pyran	*J. adhatoda*	-5.2
38	Heptasiloxane,1,1,3,3,5,5,7,7,9,9,11,11,13,13-tetradecamethyl-	*J. adhatoda*	-5.1
39	Hexasiloxane,1,1,3,3,5,5,7,7,9,9,11,11-dodecamethyl-	*J. adhatoda*	-4.7
40	Octasiloxane,1,1,3,3,5,5,7,7,9,9,11,11,13,13,15,15-hexadecamethyl-	*J. adhatoda*	-4.3
41	Pentasiloxane,1,1,3,3,5,5,7,7,9,9-decamethyl-	*J. adhatoda*	-4.3
42	Nirtetralin	*P. urinaria*	-6.9
43	Phyltetralin	*P. urinaria*	-6.9
44	Lintetralin	*P. urinaria*	-6.8
45	Hypophyllanthin	*P. urinaria*	-6.7
46	Syringin	*P. urinaria*	-6.7
47	Virgatusin	*P. urinaria*	-6.7
48	Dehydrochebulic acid trimethyl ester	*P. urinaria*	-6.6
49	Ferulic acid	*P. urinaria*	-6.5
50	5-demethoxyniranthin	*P. urinaria*	-6.5

Table 3. Continued.

No	Compound names	Plant species	Binding energy (kcal/mol)
51	Cucurbic acid	*P. urinaria*	-6.3
52	Methyl gallate	*P. urinaria*	-6.2
53	Niranthin	*P. urinaria*	-6.2
54	4-O-Methylgallic acid	*P. urinaria*	-6
55	Phyllanthin	*P. urinaria*	-5.9
56	(6r)-menthiafolic acid	*P. urinaria*	-5.9
57	4-hydroxybenzaldehyde	*P. urinaria*	-5.7
58	5-hydroxymethylfurfural	*P. urinaria*	-4.6
59	Dl-tryptophan	*S. chirayita*	-6.9
60	Gentianine	*S. chirayita*	-6.6
61	Enicoflavine	*S. chirayita*	-5.5
62	Dl-arginine	*S. chirayita*	-5.2
63	Nonacosyl_hentriacontanoate	*S. chirayita*	-5
64	Octadecanoate	*S. chirayita*	-4.8
65	Glutamate	*S. chirayita*	-4.2
66	Amorphane	*V. zizanioides*	-7
67	6,12-Epoxy-elema-1,3-diene	*V. zizanioides*	-6.9
68	13-nor-4,5-Epoxyeudesm-6-en-11-one	*V. zizanioides*	-6.9
69	Bisabolane	*V. zizanioides*	-6.7
70	3-carene	*V. zizanioides*	-6.5
71	15-nor-Funebran-3-one	*V. zizanioides*	-6.5
72	Beta-pinene	*V. zizanioides*	-6.5
73	Cis-Isoeugenol	*V. zizanioides*	-6.5
74	Cyclocopacamphan-12-al	*V. zizanioides*	-6.5
75	Isobisabolene	*V. zizanioides*	-6.5
76	Nootkatol	*V. zizanioides*	-6.4
77	Alpha-terpineol	*V. zizanioides*	-6.3
78	2-Methoxy-4-vinylphenol	*V. zizanioides*	-5.8
79	4-vinylphenol	*V. zizanioides*	-5.8
80	Eucalyptol	*V. zizanioides*	-5.8
81	Eugenol	*V. zizanioides*	-5.6
82	O-cresol	*V. zizanioides*	-5.5
83	M-cresol	*V. zizanioides*	-5.4
84	Oleamide	*V. zizanioides*	-5

Lipinski rule for validation of drug-likeness

Lipinski's rule of 5 helps to find out drug likeness of any experimental compound. Five rules are (i) molecular mass of the drug should be less than 500 Dalton, (ii) high lipophilicity (expressed as LogP less than 5), (iii) less than 5 hydrogen bond donors, (iv) less than 10 hydrogen bond acceptors, (v) molar refractivity should be between 40-130. The predictable drugs sites Lipinski Rule were checked by using SCFBio web-based database (Lipinski 2004).

Protein-protein docking

Spike glycoprotein (in free form and complex with selected phytochemicals) (Table 4) and ACE-2 were considered for protein-protein doc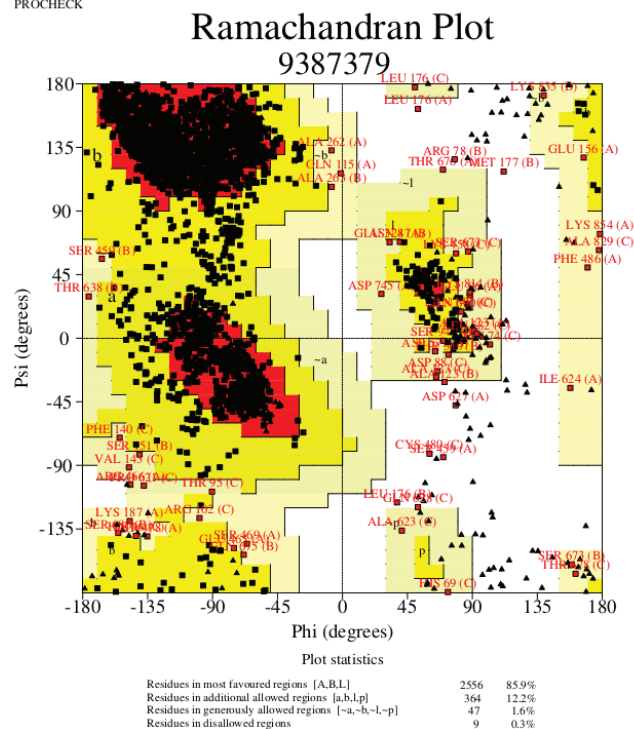king with receptor-binding domain (RBD) of the spike glycoprotein (S1 subunit) using HDOCK server (Yan et al. 2020). Precisely, the 19-41 amino acid resides of ACE-2 was employed for the docking with 417-505 amino acids of spike glycoprotein S1 subunit. In total, four ACE-2 docking experiments were performed with spike glycoprotein as per specification stated in Table 4.

RESULTS AND DISCUSSION

Homologous structure prediction of spike glycoprotein and its validation

The study of molecular docking and the ligand-based

Ramachandran Plot
9387379

Figure 1. Ramachandran plot of COVID-19 SARS-CoV-2 spike glyco-protein.

PyMol is a molecular visualization tool; used here to align the predicted three-dimensional structure of the spike glycoprotein of SARS-CoV-2 into the cryo-EM structure of 6VSB. The Root-mean-square deviation (RMSD) of this model was computed as 0.278Å. Further, the predicted 3D structure was validated through RAMACHANDRAN plot using PROCHECK. The result revealed that 85.9% belongs to the most favourable region, 12.2% in allowed region, 1.6% in the generously allowed region, and only 0.3% in disallowed region (Fig. 1). Though cryo EM structure of SARS-COV-2 spike glycoprotein (6VSB) was available, some amino acids were not resolved properly at different locations due to its 3.46 Å resolution. To get the complete structure of spike, homology modelling was performed. Good quality structure with 98.1% residues at ordered form indicated the proper conformational packaging of protein.

Assessment of binding affinity of 213 ligands with spike protein and their subsequent screening

A spike glycoprotein of SARS-COV-2 has three domains namely S1, S2 and N. The S2 domain intercedes the membrane fusion process and the S1 domain utilizes human angiotensin-converting enzyme-2 (hACE-2) as the receptor to infect human cells (Pandey et al. 2020). The literature review revealed that the receptor-binding domain (RBD) of the S1 subunit of spike protein binds with the target cell ACE-2 receptor and forms the RBD-ACE-2 complex. According to recent report, ACE-2 could mediate SARS-CoV-2 binding by spike protein key residues of K417, G446, Y449, F486, N487, Y489, Q493, Q498, T500, N501, G502, Y505 (Walls et al. 2020; Wang et al. 2020; Yan et al. 2020; Lan et al. 2020). In this in-silico study, we attempted to explore the binding affinity of 213 phytochemicals in addition to remdesivir, lopinavir, chloroquine and hydroxychloroquine with the active site residues of the spike glycoprotein (Fig. 2A). The selection of the natural ligands of plant origin was primarily made on the basis of (i) minimal binding energy (<-7 kcal/mol) and (ii) formation of at least one H-bond with the active site residues (417-505) in the S1 subunit of the spike glycoprotein. These criteria were fulfilled by 23 compounds which were further blindly docked with whole spike glycoprotein

computer-aided drug discovery approach involves energy, affinity and three-dimensional structural conformations-based analysis of ligands interaction with the target of interest. The binding ability of a ligand molecule to a specific target site depends on occurrence of proper cleft, proper hydrogen bonding and the nature of residues present at the target site and their interactive energy balance (Tripet et al. 2004). The binding affinity of a ligand for a targeted receptor is measured by binding energy. Lower binding energy implies that binding affinity is high whereas higher energy endorses the reverse (Zhou et al. 2020). In the present study, three-dimensional (3D) homologous structure of spike glycoprotein was generated from the reference protein sequence (YP_009724390.1) using the cryo-EM structure (6VSB) through SWISS-MODEL server and further analyzed through PyMol.

Table 4. Different complex of spike glycoprotein (free and ligand bound) and ACE2 docking in HDOCK and their binding score.

Molecular docking complex	HDOCK score	RMSD value
Spike glycoprotein dock with ACE2	-360.86	*0.51*
Spike glycoprotein and rhamnocitrin dock with ACE2	-360.86	*0.51*
Spike glycoprotein and 1,5-dihydroxy-3,8-dimethoxyxanthone dock with ACE2	-243.15	*481.28*
Spike glycoprotein and laevojunenol dock with ACE2	-238.13	*480.02*

Table 5. Physicochemical properties of natural plant derived compounds and their binding energy during molecular docking. Different capital alphabets before amino acids indicate different polypeptide chains.

Compound name	Amino acids at docked sites	Lipinski criteria for drug-likeness				
		MW (g/mol)	Hydrogen bond donor	Hydrogen bond acceptor	XLogP3-AA	Molar refractivity
Rhamnocitrin	B/PHE-490, B/SER-477, C/SER-371, B/ARG-457,	300.26	3	6	2.2	77.272881
1,5-dihydroxy-3,8-dimethoxyxanthone	B/GLU-406, B/GLN-409, B/LYS-417	288.26	2	6	2.37	77.145782
Laevojunenol	B/TYR-489	222.37	1	1	3.78	77.145782

(Table 1-2) to analyze the affinity of selected molecules at the active site of spike glycoprotein (417-505) instead of other cleft and pockets. It was evident that rhamnocitrin of *P. urinaria*, 1,5-dihydroxy-3,8-dimethoxyxanthone of *S. chirayita*, laevojunenol and khusinol of *V. zizanioides* are capable to bind with active site residues of the S1 subunit of spike glycoprotein (S) in 0 (zero) RMSD pose (Fig. 2). So, these three phytochemicals are the best ligand molecules for spike protein active site which restricts smooth interaction between spike and ACE-2.

The molecular docking study of spike protein with remdesivir revealed that this drug has the capability to bind with S1 domain through H-bond with the ARG403, ASP405 and ARG408 of B and PHE374, SER375 and TYR508 of C chain with binding energy of -8.1 kcal/mol. However, though remdesivir binds with the spike protein at S1 domain, but the site of attachment is not

the active site of spike protein. Lopinavir interacts with the S2 subunit through amino acid residues GLN957, THR961 and associated with binding energy of -11.8 kcal/mol. Alongside, it was also revealed that chloroquine and hydroxychloroquine binds with LEU455, GLY485, PHE490, PRO491 and PRO559, PHE855, THR573, ILE587 residues of S2 domain having the binding energy of -6.7 and -6.3 kcal/mol, respectively (Table 3). It is evident that among the four drugs neither one is capable to bind at active site of spike glycoprotein.

The docking results were analysed based on a combination of binding energy, clustering score, shape complementarity, functional significance of the binding pocket and favourable interactions including H bonds.
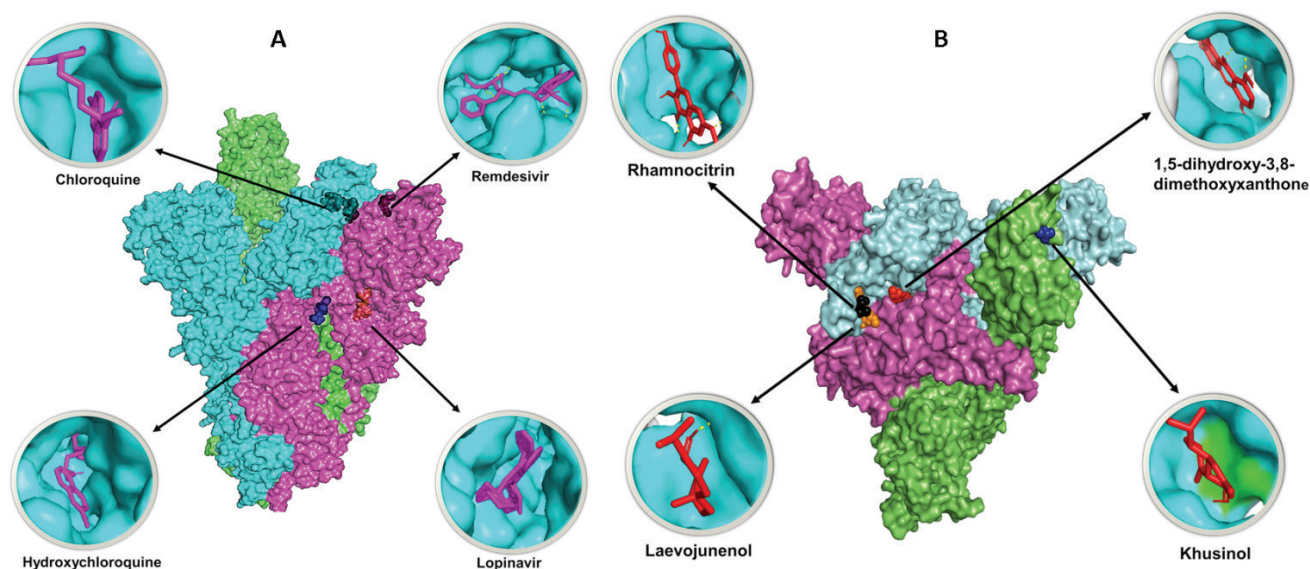
Figure 2. Binding of (A) remdesivir, lopinavir, chloroquine and hydroxychloroquine and (B) rhamnocitrin, 1,5-dihydroxy-3,8-dimethoxyxanthone, laevojunenol and khusinol with SARS-CoV-2 spike glycoprotein.
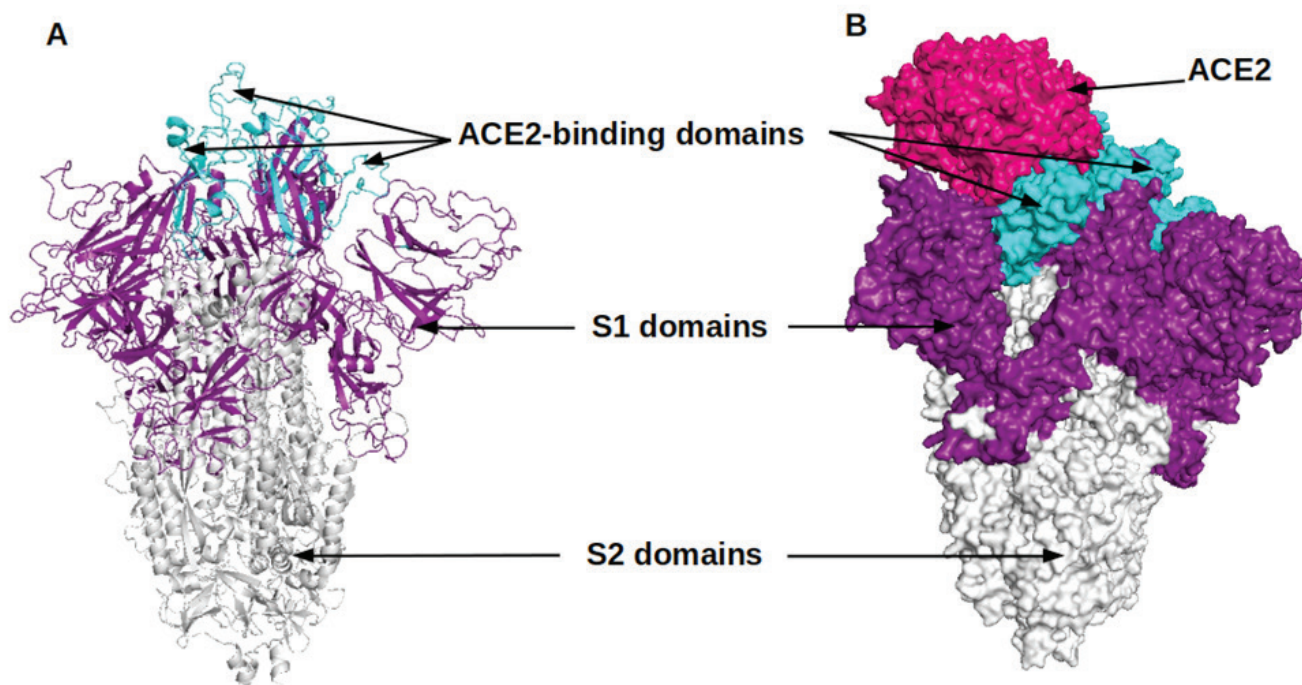
Figure 3. Binding of hACE2 with SARS-CoV-2 spike glycoprotein. (A) cartoon view and (B) surface view.

Validation of drug-likeness

Lipinski rule of five is a rule of thumb to check the drug's likeness of any chemical compound. It acts as a filter to screen potential therapeutic agents/drugs just at the initiation of the program, thereby minimizing the labour and costs of clinical drug development and to a large extent prevents late-stage clinical failures (Raj et al. 2019; Pandey et al. 2020). In this study, three selected phytochemicals were examined for their drug-likeness in the light of the rules (Table 5). The results clearly demonstrated that rhamnocitrin, 1,5-dihydroxy-3,8 dimethoxyxanthone and laevojunenol qualified the rule.

Ligand binding effect analysis on spike glycoprotein-ACE-2 interaction

Finally, the selected drugs were individually used to study effective inhibition of RBD-ACE2 complex formation. The interaction of spike glycoprotein with ACE-2 is depicted in Fig. 3. In order to verify the possible effect of the ligands in spike-ACE-2 interaction, the S glycoprotein-ligand docked complexes were further docked with ACE-2 protein in HDOCK web server. HDOCK is a web server-based protein-protein and protein-DNA/RNA docking tool. This web server based molecular docking revealed that the binding energy of spike protein-ACE-2 interaction was −360.86 and rmsd value 0.51 which decreased to -243.15 and 481.28 rmsd for 1,5-dihydroxy-3,8-di-methoxyxanthone, -238.13 and 480.02 for laevojunenol,

-360.86 and 0.51 for rhamnocitrin separately pre-fixed with spike glycoprotein, respectively. Apart from the effect on binding energy, it was also evident that the binding of 1,5-dihydroxy-3,8-dimethoxyxanthone and laevojunenol triggers the shifting of interaction sites of both the partners from their active sites which may hamper the viral entry into human cell (Fig. 4). Also 1,5-dihydroxy-3,8-dimethoxyxanthone of *S. chirayita*, laevojunenol of *V. zizanioides* binding pose being poor, these compounds can be considered as potential inhibitor of S-glycoprotein and human ACE-2 interaction.

CONCLUSION

In conclusion, we can state that the present computer-aided *in-silico* study of exploration of preventive drugs against COVID-19 revealed that natural herbal phytochemicals like rhamnocitrin; 1,5-dihydroxy-3,8-dimethoxyxanthone and laevojunenol of *P. urinaria*, *S. chirayita*, and *V. zizanioides* have immense potential to restrict the onset of SARS-COV-2 disease due to their ability to interrupt the normal viral spike protein and ACE-2 interaction upon binding to the spike protein. The potential of 1,5-dihydroxy-3,8-dimethoxyxanthone and laevojunenol was proved to be superior. Maybe these compounds will be useful as potential preventive drugs, however, further experiments are necessary to validate their effects.
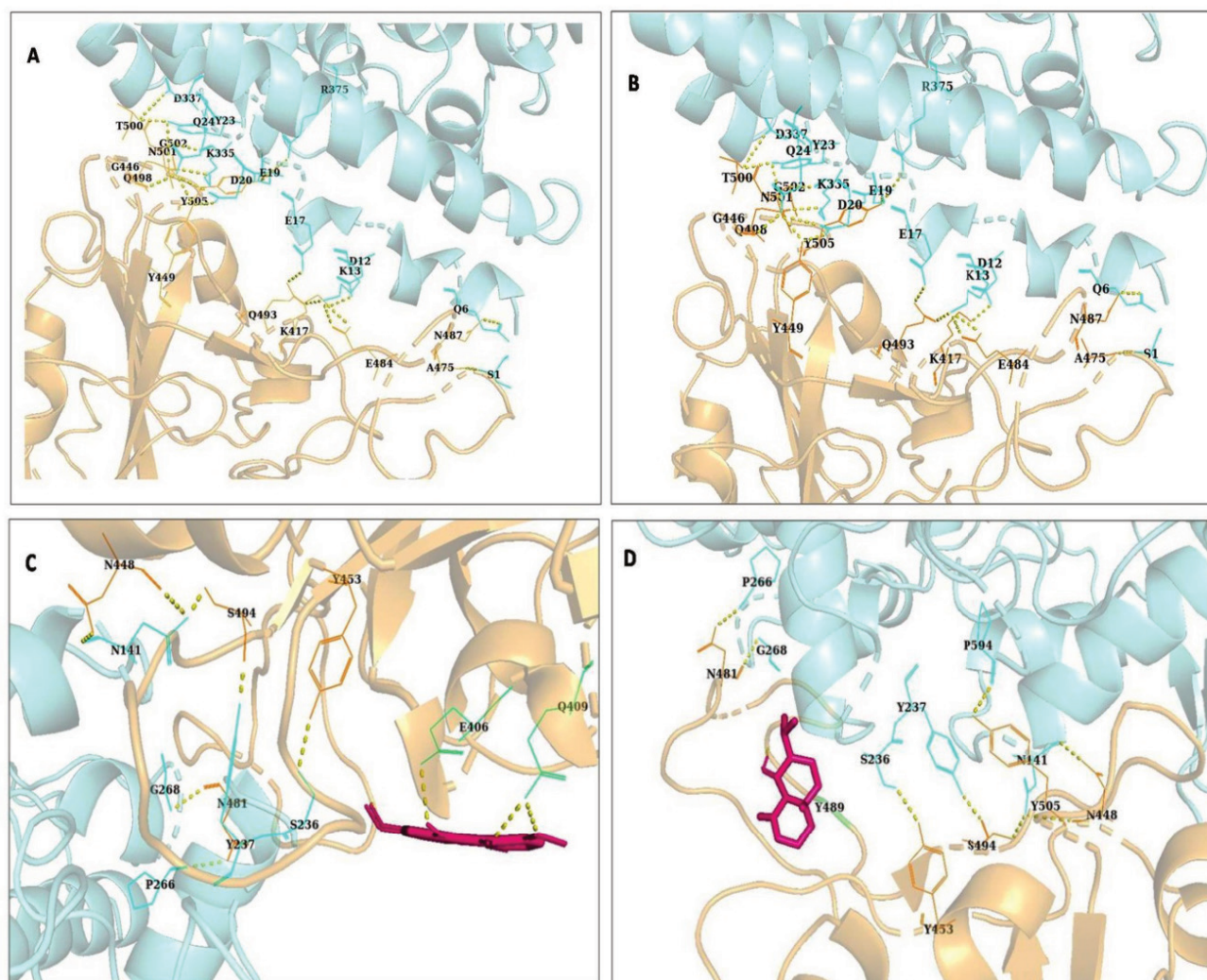
Figure 4. Spike protein bound with ACE2 in open condition (A). Binding of hACE2 with SARS-CoV-2 spike glycoprotein already bound 1,5-dihydroxy-3,8-dimethoxyxanthone (C) and laevojunenol (D). Change in binding position between hACE2 with SARS-CoV-2 spike glycoprotein was apparent in case of all except rhamnocitrin (B).

Acknowledgement

References

Bourgonje AR, Abdulle AE, Timens W, Hillebrands JL, Navis GJ, Gordijn SJ, Bolling MC, Dijkstra G, Voors AA, Osterhaus AD, van der Voort PH (2020) Angiotensin-converting enzyme-2 (ACE2), SARS-CoV-2 and pathophysiology of coronavirus disease 2019 (COVID-19). J Pathol 251(3):228-248.

Cao B, Wang Y, Wen D, Liu W, Wang J, Fan G, Ruan L, Song B, Cai Y, Wei M, Li X (2020) A trial of lopinavir–ritonavir in adults hospitalized with severe Covid-19. N Engl J Med 382:1787-1799.

DeLano WL (2002) Pymol: An open-source molecular graphics tool. CCP4 Newslett Prot Crystallogr 40(1):82-92.

Dev S (1999) Ancient-modern concordance in Ayurvedic plants: some examples. Environ Health Perspect 107(10):783-789.

Divya M, Vijayakumar S, Chen J, Vaseeharan B, Durán-Lara EF (2020) A review of South Indian medicinal plant has the ability to combat against deadly viruses along with COVID-19? Microb Pathog 104277.

Jaiswal YS, Williams LL (2017) A glimpse of Ayurveda–The forgotten history and principles of Indian traditional

medicine. J Tradit Compl Med 7(1):50-53.

Kim S, Thiessen PA, Bolton EE, Chen J, Fu G, Gindulyte A, Han L, He J, He S, Shoemaker BA, Wang J (2016) PubChem substance and compound databases. Nucleic Acids Res 44:D1202-D1213.

Koparde AA, Doijad RC, Magdum CS (2019) Natural products in drug discovery. In Pharmacognosy-Medicinal Plants. IntechOpen.

Kuba K, Imai Y, Rao S, Gao H, Guo F, Guan B, Huan Y, Yang P, Zhang Y, Deng W, Bao L (2005) A crucial role of angiotensin converting enzyme 2 (ACE2) in SARS coronavirus–induced lung injury. Nat Med 11(8):875-879.

Kumar V, Van Staden J. (2015) A review of *Swertia chirayita* (Gentianaceae) as a traditional medicinal plant. Front Pharmacol 6:308.

Lan J, Ge J, Yu J, Shan S, Zhou H, Fan S, Zhang Q, Shi X, Wang Q, Zhang L, Wang X. (2020) Structure of the SARS-CoV-2 spike receptor-binding domain bound to the ACE2 receptor. Nature 581(7807):215-220.

Laskowski RA, MacArthur MW, Moss DS, Thornton JM (1993) PROCHECK: a program to check the stereochemical quality of protein structures. J Appl Cryst 26(2):283-291.

Lipinski CA. (2004) Lead-and drug-like compounds: the rule-of-five revolution. Drug Discov Today Technol 1(4):337-341.

Lavanya P, Ramaiah S, Anbarasu A (2016) Ethyl 4-(4-methylphenyl)-4-pentenoate from Vetiveriazizanioides inhibits dengue NS2B–NS3 protease and prevents viral assembly: a computational molecular dynamics and docking study. Cell Biochem Biophys 74:337-351.

Mohanraj K, Karthikeyan BS, Vivek-Ananth RP, Chand RB, Aparna SR, Mangalapandi P, Samal A (2018) IMPPAT: A curated database of Indian Medicinal Plants, Phytochemistry and Therapeutics. Sci Rep 8(1):4329.

Pandey P, Rane JS, Chatterjee A, Kumar A, Khan R, Prakash A, Ray S (2020) Targeting SARS-CoV-2 spike protein of COVID-19 with naturally occurring phytochemicals: an in-silico study for drug development. J Biomol Struct Dyn 22:1-11.

Paramanick D, Panday R, Shukla SS, Sharma V (2017) Primary pharmacological and other important findings on the medicinal plant *"Aconitum heterophyllum"* (aruna). J Pharmacopunct 20(2):89-92.

Raj S, Sasidharan S, Dubey VK, Saudagar P (2019) Identification of lead molecules against potential drug target protein MAPK4 from *L. donovani*: An *in-silico* approach using docking, molecular dynamics and binding free energy calculation. PloS One 14(8):e0221331.

Rajeswara Rao BR (2013) Biological activities and medicinal uses of the essential oil and extracts of lemongrass (*Cymbopogon flexuosus, C. citratus, C. pendulus* and *C. species*). In Govil JN, Bhattacharya S, Eds., Recent Progress

in Medicinal Plants: Essential Oils I. Vol. 36. Studium Press LLC, Houston, USA. pp. 213-257.

Rismanbaf A, Zarei S (2020) Liver and kidney injuries in COVID-19 and their effects on drug therapy; a letter to editor. Arch Acad Emerg Med 8(1):e17.

Singh DD (2018) Assessment of antimicrobial activity of hundreds extract of twenty Indian medicinal plants. Biomed Res 29(9):1797-1814.

Suresh A, Abraham J (2020) Phytochemicals and their role in pharmaceuticals. In Patra J, Shukla A, Das G, Eds., Advances in Pharmaceutical Biotechnology. Springer, Singapore. pp. 193-218.

Tripet B, Howard MW, Jobling M, Holmes RK, Holmes KV, Hodges RS (2004) Structural characterization of the SARS-coronavirus spike S fusion protein core. J Biol Chem 279(20):20836-20849.

Trott O, Olson AJ (2010) AutoDock Vina: improving the speed and accuracy of docking with a new scoring function, efficient optimization, and multithreading. J Comput Chem 31(2):455-461.

ul Qamar MT, Alqahtani SM, Alamri MA, Chen LL (2020) Structural basis of SARS-CoV-2 3CLpro and anti-COVID-19 drug discovery from medicinal plants. J Pharm Anal 10(4):313-319.

WHO Coronavirus Disease (COVID-19) Dashboard (https://covid19.who.int/) [accessed 13 January 2021].

Walls AC, Park YJ, Tortorici MA, Wall A, McGuire AT, Veesler D (2020) Structure, function, and antigenicity of the SARS-CoV-2 spike glycoprotein. Cell 181(2):281-292.

Wang Q, Zhang Y, Wu L, Niu S, Song C, Zhang Z, Lu G, Qiao C, Hu Y, Yuen KY, Wang Q (2020) Structural and functional basis of SARS-CoV-2 entry by using human ACE2. Cell 81(4):894-904.

Waterhouse A, Bertoni M, Bienert S, Studer G, Tauriello G, Gumienny R, Heer FT, de Beer TA, Rempfer C, Bordoli L, Lepore R (2018) SWISS-MODEL: homology modelling of protein structures and complexes. Nucleic Acids Res 46(W1):W296-303.

Yan R, Zhang Y, Li Y, Xia L, Guo Y, Zhou Q (2020) Structural basis for the recognition of SARS-CoV-2 by full-length human ACE2. Science 367(6485):1444-1448.

Yan Y, Tao H, He J, Huang SY (2020) The HDOCK server for integrated protein–protein docking. Nat Protoc 15(5):1829-1852.

Yang XH, Deng W, Tong Z, Liu YX, Zhang LF, Zhu H, Gao H, Huang L, Liu YL, Ma CM, Xu YF (2007) Mice transgenic for human angiotensin-converting enzyme 2 provide a model for SARS coronavirus infection. Comp Med 57(5):450-459.

Yao X, Ye F, Zhang M, Cui C, Huang B, Niu P, Liu D (2020) In vitro antiviral activity and projection of optimized dosing design of hydroxychloroquine for the treatment of severe acute respiratory syndrome coronavirus 2

(SARS-CoV-2). Clin Infect Dis 71(15):732-739.

Yazdany J, Kim AH (2020) Use of hydroxychloroquine and chloroquine during the COVID-19 pandemic: what every clinician should know. Ann Int Med 172(11):754-755.

Zhou P, Yang XL, Wang XG, Hu B, Zhang L, Zhang W, Si HR, Zhu Y, Li B, Huang CL, Chen HD (2020) A pneumonia outbreak associated with a new coronavirus of probable bat origin. Nature 579(7798):270-273.